Maximum Receiver Harvesting Area of Backscatter Signals from Ambient Low-Frequency Mobile Networks

Ritayan Biswas, Joonas Säe, Jukka Lempiäinen
Faculty of Information Technology and Communication Sciences (ITC), Tampere University, 33720 Tampere, Finland
Email: {ritayan.biswas, joonas.sae, jukka.lempiainen}@tuni.fi

***Abstract*—The purpose of this paper is to estimate the maximum achievable range for ambient backscattering communications (AmBC) by utilizing one of the lowest available frequency bands for mobile networks. Long term evolution (LTE) networks operating at 700 MHz (LTE-700, also referred to as LTE band 28) use the frequency division duplexing (FDD) technique for communications and are utilised as the ambient signals to perform the simulations. The simulations are carried out in urban macro-cellular and suburban highway environments. For the simulations, the sensors are placed in the line-of-sight (LOS) path of the LTE-700 transmitter and receiver antenna as this ensures the maximum applicability of the AmBC technology. Two propagation models, the ray tracing approach and the radar equation are leveraged to determine the maximum range of communication when the signal is reflected by the sensor. It is observed from the analysis that distances of a few hundred meters are achievable utilising both propagation models. The size of the sensor has a pivotal role in determining the maximum range of communication while utilising the radar equation. Therefore, a thorough analysis is performed using real-world sensor sizes deployed for the internet of things (IoT) wireless communication.**

***Index Terms*—Internet of Things, Sensor, Radar cross section, AmBC, LTE, 5G.**

I. Introduction

Ambient backscattering communications (AmBC) is a wireless communication technology which utilises ambient radio frequency (RF) signals to establish communication with sensors or devices. These sensors have their applicability in the internet of things (IoT) wireless communications. These ambient signals can originate from a variety of RF sources such as television (TV) broadcasts, Wi-Fi, FM radio and cellular signals. The sensors used in AmBC are capable of harvesting energy from the ambient RF signals. This enables the battery free and wireless operation of the sensors.

AmBC systems operate on the principle of radio backscatter where a transmitted signal is reflected back from an object towards a receiver for decoding. This technique was first utilized during World War II to determine the identity of the air-crafts and classify then as friendly or hostile. The first article on backscatter communications was published by Harry Stockman in 1948 [1]. There has been a significant amount of research in the radio backscatter technology during the last two decades due to the relatively low cost and very low power requirement of manufacturing such devices [2]. Radio frequency identification (RFID) systems also utilize the concept of radio backscatter in order to perform their functionality.

The concept of AmBC was first presented by the authors of [3] in the year 2013. They were able to achieve communication distances of $45.7\,\mathrm{cm}$ in indoor environments and $76.2\,\mathrm{cm}$ in outdoor environments by utilising ambient TV broadcast signals [3]. Backscatter communication utilising ambient wireless LAN (WLAN) signals were presented by the authors in [4]. They were able to connect to the internet by connecting to the gateway network [4]. There was a significant improvement in throughput achieved in [5] in comparison with previous articles such as [3], [4]. Typically, it was observed that very short communication ranges could be achieved by AmBC systems. However, in [6], wide area communication was proposed for AmBC and it was predicted that communication distances of $30\,\mathrm{km}$ are achievable utilizing ambient FM radio signals based on power budget calculations. Furthermore, the link budget for typical backscatter communications at different frequencies were studied by the authors in [7].

In this article, ambient long term evolution (LTE) cellular signals operating at $700\,\mathrm{MHz}$ (LTE-700) frequency are utilised to estimate the maximum distance between the TX/RX antenna and the sensor in outdoor environments. To maximise the coverage, the LTE-700 carrier frequency band is utilised as this is one of the lowest operating frequencies for cellular communications. Additionally, the simulations are performed for the sensors located in the direct line-of-sight (LOS) of the TX/RX antenna in urban macro-cellular and suburban highway environments. Furthermore, the TX and the RX are placed in the same location which represents the mono-static mode of operation for AmBC systems. The simulation results demonstrate that the AmBC systems are capable of achieving distances of the order of hundreds of meters when typical real world antenna configurations are utilised.

II. Backscatter Communications

Backscatter systems can be classified into two categories based on the location of the TX and RX. In the mono-static mode of operation, the TX and RX are placed in the same location. The signal transmitted by a dedicated TX

reflects back from an object (or, sensor) towards the RX for detection [8]. The bi-static backscatter utilizes a carrier emitter to transmit a dedicated signal to the sensor which is backscattered to a RX for reading and decoding the signal [8]. This type of system can utilize a centrally located receiving device capable of decoding the signal [9]. However, a disadvantage of traditional backscatter communication systems is the requirement for a dedicated transmission.

AmBC eliminates the need of a dedicated signal by utilising the ambient RF signals present in the environment. These ambient signals can be transmitted from a variety of sources such as TV/FM broadcasts, WLAN or cellular signals to name a few. These ambient signals are utilized by the backscattering element in order to establish communication between two passive or active devices or a combination of both. The advent of IoT wireless communication necessitates the deployment of a huge number of sensors. All these sensors will have a power requirement as they are required to communicate with each other or other devices. However, it might impractical to change batteries for certain use cases and in some environments [3], [10]. Therefore, the harvesting of energy from ambient RF signals is an important feature ensured by AmBC [11].

The operating principle of the AmBC technology is based on the transmission of "1" or "0" from the sensor. For example, "1" can indicate the reflecting state and "0" can indicate the non-reflecting state [11]. In order to establish communication, the antenna impedance states are changed between the non-reflecting and reflecting states [3]. The signal transmitted from the chosen ambient RF source propagates to the sensor, where the signal is modulated and forwarded to a device capable of receiving and decoding the signal.

Although AmBC has significant advantages, there are some practical disadvantages that need to be addressed before commercial deployment is possible. Firstly, the RX/sensors must be capable in deciphering between various RF signals emitted from legacy sources. Secondly, the capability of energy harvesting at the sensor will be a challenge for hardware designers. Lastly, the mode of operation of AmBC differs from traditional wireless communications. Therefore, separate channels need to be defined for communication utilizing ambient RF signals in comparison with traditional communication systems.

III. Propagation models

To examine the signal path from the TX antenna to the sensor, each environment is analysed with the help of two propagation models. While performing the analysis, the signal is assumed to have a clear LOS between the TX antenna, RX antenna and the sensor.

A. Radar Equation

The radar equation (RE) generally computes the total range of communication. The operating principle of the radar equation is based on the reflection of the transmitted signal from the target of a given cross section back to the RX antenna. The radar can be mono-static, that is, the TX and RX is positioned at the same location. In bi-static radar, the signal travels from the TX via reflection from a target to the RX antenna which are not collocated. In this work, mono-static radar is considered for computing the range. The formula for the computation of the range using the radar equation is shown in (1).

$$R = \sqrt[4]{\frac{P_t G_t G_r \lambda^2 \sigma}{(4\pi)^3 P_r L}}. \tag{1}$$

The range from the TX antenna to the sensor is expressed by R_t, and R_r represents the range of the sensor to the RX antenna. For mono-static radar two ranges are nearly identical and can be combined into R [12]. These distances are expressed in meters. Parameters such as wavelength (λ), transmit power (P_t) and the antenna gains of the TX (G_t) and RX (G_r) has a vital role in determining the range of radar systems. L represents the propagation loss of the system. The received power (P_r) indicates the receiver sensitivity (or, noise floor) and is calculated using (2),

$$RX_{\text{sensitivity}}(\text{dBm}) = 10 \cdot \log_{10}\left(\frac{kTB}{0.001}\right) + NF + SNR. \tag{2}$$

The values for the parameters represent typical values used for the LTE power budget calculation. The temperature (T) is 290 K and Boltzmann's constant (k) is 1.38×10^{-23} J/K. For calculating the bandwidth (B), one resource block ($12 \times 15\,\text{kHz}$) is utilized. The number of sub-carriers is 12 and the spacing between them is $15\,\text{kHz}$ [13].

The cross section of the target (sensor, σ) is expressed in square meters and plays an important role in in the operation of the radar. In literature [12], the value of σ is calculated using (3),

$$\sigma = 0.88 \times \lambda^2, \tag{3}$$

when the antenna is considered to be a half dipole. The wavelength is calculated to be $0.42\,\text{m}$ for $700\,\text{MHz}$.

B. Ray Tracing

The ray tracing (RT) approach is generally based on the comprehensive simulation of the propagation environment. A proper description of the physical propagation environment is necessary in order to provide a deterministic representation of the ray path(s). The simulation is carried out by using rays to model different multi-path components of the environment in detail. The total ray paths are subdivided into LOS links. The propagation of the individual LOS link between two points is determined by the free space path loss (FSPL) utilizing (4).

$$FSPL = 32.45 + 20 \cdot \log_{10}(d_{\text{km}}) + 20 \cdot \log_{10}(f_{\text{MHz}}), \tag{4}$$

where d represents the distance (in km) between the two points and f represents the frequency (in MHz) of operation.

Generally, in an environment each ray experiences reflection, diffraction and/or scattering which can be termed as

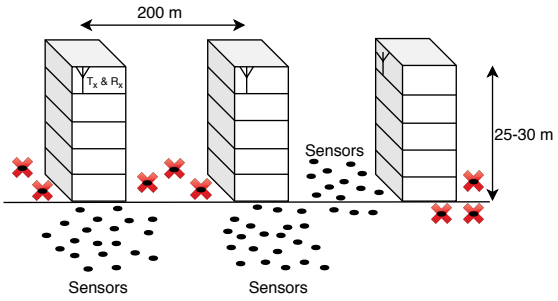

Fig. 1. Urban macro-cellular environment.

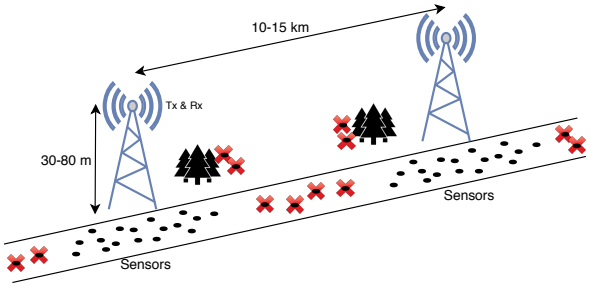

Fig. 2. Sub-urban highway environment.

the propagation loss. The total loss experienced by a certain ray is a combination of these phenomena and the loss due to the distance traveled by the signal. In order to obtain an accurate prediction of the propagation, the parameters that affect the ray tracing approach are thoroughly analysed. Building penetration losses, the permittivity of the ground and building materials, the precise locations of the TX antenna, RX antenna and the obstacles (buildings, trees) need to be accurately modelled. Losses occurring due to any of these phenomena contribute to the propagation loss. The final result is a combination of the FSPL for each individual LOS link of the ray in addition to the propagation loss. Additionally, the frequency of operation also has an important role in the simulation. The received signal power is computed based on the multi-path components that exist between the TX antenna and the RX antenna.

IV. Computation of the Receiver Harvesting Area

The receiver harvesting area is determined based on the simulation performed in two different environments, an urban macro-cellular and a suburban highway environment.

A. Environment for receiver harvesting area

The harvesting area of the receiver is determined based on the location of the sensor relative to the TX/RX. Additionally, the strength of the reflected signal also determines the area where the sensors can be deployed. This study is focused on the analysis of urban macro-cellular environment and suburban highway environment where there are direct LOS paths between the TX/RX and the sensor. It is assumed the transmitter and the receiver are placed at the same location. Therefore, the signal travels from the transmitter to the sensor and back to the receiver following the same path. Additional losses due to reflection and scattering are included while computing the total path loss. The sensors are placed at the ground level or at heights of $1\,\mathrm{m}$ from the ground in the direct LOS path of the transmitter. Thus, some additional loss is also considered for the obstruction caused by the blocking of the Fresnel zone.

1) Urban macro-cellular environment: In the urban macro-cellular environment, there are clear LOS paths present between the TX antenna and the sensor. The sensors which are located in the non line-of-sight (NLOS) with respect to the TX antenna are unable to receive and harvest the signals. These sensors are marked with red crosses in Fig. 1. Generally, in an urban macro-cellular environment the TX is located on or just below the rooftop. In this work, the location of the TX is considered to be just below the rooftop level (as depicted in Fig. 1) in order to avoid the back-lobe of the antenna radiation pattern. Also, by placing the antenna just below the rooftop level, the signal in the main beam direction is emphasised in the direct LOS with the sensor. In this work, the RX is placed at the same location of the TX at a height of $30\,\mathrm{m}$. The inter-site distance in a standard urban macro cellular environment is $200\,\mathrm{m}$. The illustration of the propagation environment for such a scenario is depicted in Fig. 1.

2) Suburban highway environment: The height of the TX antenna in a suburban highway environment is typically between $30\,\mathrm{m}$ to $80\,\mathrm{m}$. The cost efficient way is to have the TX as high as possible. This is done in order to have the maximum possible coverage and avoid the nearby obstacles such as trees. It is assumed RX antenna is located at the same height of the TX antenna. The sensors are placed near the TX ensuring a clear LOS path. The location of these sensors is depicted in Fig. 2. The sensors which are in the NLOS of the TX are represented in Fig. 2 with red crosses. The typical site distances for a highway environment is $10\,\mathrm{km}$ to $15\,\mathrm{km}$. This signifies there are parts of the highway between TX where the sensors cannot be deployed. A schematic diagram for the receiver harvesting area in a highway environment is illustrated in Fig. 2.

B. Simulation parameters

The analysis of the signal propagation in the urban macro-cellular and highway LOS environments is performed utilizing the radar equation and the ray tracing method. The sensors are located in the direct LOS of the TX/RX and an illustration of two environments are shown in Fig. 1 and Fig. 2.

The effective isotropic radiated power (EIRP) of the LTE-700 TX antenna is $62\,\mathrm{dBm}$. This is calculated based on a transmit power (P_t) of $46\,\mathrm{dBm}$ (typical for most manufacturers), a transmit antenna gain (G_t) of $18\,\mathrm{dB}$ and a cable loss of $2\,\mathrm{dB}$. The noise figure (NF) is $10\,\mathrm{dB}$ and the signal to noise ratio (SNR) is $2\,\mathrm{dB}$. These values indicate typical values utilised in the LTE power budget calculations. The value of the receiver sensitivity is calculated to be

TABLE I
SIMULATION PARAMETERS.

Parameter	Unit	Value
TX power (P_t)	dBm	46
TX antenna gain (G_t)	dBi	18
RX antenna gain (G_r)	dBi	0
Cable loss	dB	2
Temperature (T)	K	290
Bandwidth (B)	kHz	12×15
Noise figure (NF)	dB	10
Signal-to-noise ratio (SNR)	dB	2
Additional loss (urban, L_{urban})	dB	15
Additional loss (suburban, L_{suburban})	dB	5

$-109.42\,\text{dBm}$ utilising (2). Therefore, the total available path loss is $171.42\,\text{dB}$ based on the difference between the EIRP and the receiver sensitivity.

The free space path loss is calculated for the LOS link between the TX/RX and the sensor utilizing equation (4). The total path loss is a summation of the path loss between the TX and sensor and the path loss between the sensor and RX after reflection (from the sensor). In the urban environment, there is approximately $15\,\text{dB}$ additional loss (L_{urban}) considered due to the reflection off the sensor ($10\,\text{dB}$) and the minor obstruction of the first Fresnel zone ($5\,\text{dB}$). The total additional loss (L_{suburban}) in suburban environment is approximately $5\,\text{dB}$. In equation (1), the additional loss values are utilized for the L term. P_r (or, the receiver sensitivity) determines the minimum value of the signal strength that can be received at the RX. A comparison is performed for two approaches in order to determine the feasibility of these propagation models for this approach. The different parameters utilised for the simulations are summarised in the table I.

V. RESULTS AND ANALYSIS

The total available loss that an individual ray can experience in the LOS path is $156.42\,\text{dB}$ in urban and $166.42\,\text{dB}$ in suburban environments, respectively. These values are calculated after the additional loss for the respective environments are considered as stated in table I. The available path loss is basically the round-trip loss experienced by the ray when it travels from the TX to the sensor, gets reflected and travels back to the RX.

Utilizing the ray tracing method it is observed that a maximum distance of approximately $275\,\text{m}$ can be achieved between the TX and the sensor in the clear LOS link in urban environments. The FSPL at a distance of $275\,\text{m}$ from the TX is $78.14\,\text{dB}$ utilizing (4). Based on the principle of reciprocity, the path between the sensor and the RX experiences a similar path loss. Thus, the total path loss experienced by the signal is $156.28\,\text{dB}$ which is less than the maximum allowable loss for the urban environment after the additional loss is taken into account. Therefore, theoretically, a signal in the LOS path can travel $550\,\text{m}$ between the TX and the RX via reflection from the sensor. In the urban macro-cellular environment, the sensors can be placed approximately $275\,\text{m}$ away from the TX/RX antenna in the clear LOS path in order to perform various functionalities based on different use cases. The site distances in an urban environment is about $200\,\text{m}$ therefore most of the sensors are able to utilize the ambient signals. The urban macro-cellular environment represents the worst case for distance calculations due to the large amount of interference in this type of environment.

TABLE II
DIFFERENT DISTANCES FOR AMBC WITH RT AND RE PROPAGATION MODELS.

Propagation model	RCS (σ, m^2)	Urban Total distance (m)	Sub-urban Total distance (m)
Ray Tracing	-	550	950
Radar equation	0.001	159	283
	0.01	283	503
	0.16	567	1000
	0.3	662	1178
	0.7	819	1456

Similarly, a signal is able to travel $475\,\text{m}$ between the TX and the sensor in a suburban environment when a LOS link exists between them. The loss at a distance of $475\,\text{m}$ is $82.29\,\text{dB}$. Therefore, a total loss of $164.58\,\text{dB}$ is experienced by a signal travelling from the TX to the RX via reflection from the sensor. As this value is less than the total available loss, a communication link of $950\,\text{m}$ between the TX and the RX can be established after the signal is reflected from the sensor. In the highway environment, the sensors can be placed within a diameter of $0.95\,\text{km}$ centering around the TX. The site distances in highway environments are about $10\,\text{km}$ to $15\,\text{km}$ so all the sensors need to be placed in the vicinity of the TX/RX. As the interference and the additional loss is less in comparison, greater distances can be achieved by the ambient signal. Therefore, due to the lower losses experienced in highway environments these results are optimistic. Sensors located in the NLOS path of the TX/RX experience greater losses and further studies and measurements need to be performed to determine how coverage can be provided to them.

The range (R, km) is calculated utilizing the radar equation (1) using different values for the radar cross section (σ). The values considered for σ attempts to indicate the size of the sensors used in IoT wireless communications. The worst case scenario is when the value of σ is the smallest as the signal has the least surface area to reflect back from.

In the urban macro-cell environment, a total distance of $159\,\text{m}$ can be achieved when utilising a sensor of $0.001\,\text{m}^2$. The total achievable range of communication is $283\,\text{m}$ when a $0.01\,\text{m}^2$ is used. A distance of $567\,\text{m}$ is achievable when a half-dipole antenna (σ = $0.16\,\text{m}^2$) is used (based on the value calculated using (3). This distance represents the most realistic value when compared with the ray tracing technique. Longer communication distances of $662\,\text{m}$ and $819\,\text{m}$ are

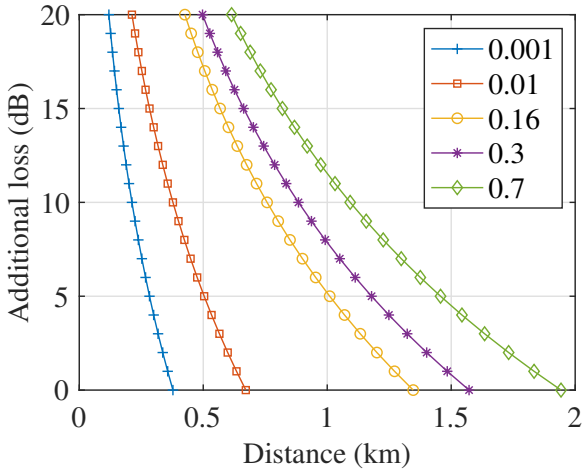

Fig. 3. Achievable distances for different system and additional losses for varying RCS (σ).

achievable when $0.3\,\mathrm{m}^2$ and $0.7\,\mathrm{m}^2$ sensors are utilised, respectively. However, such sensor sizes may be impractical in practical applications. The large sensors indicate the best case scenario as the signal has a much larger surface to reflect back from. A $15\,\mathrm{dB}$ additional loss is used for these calculations and the summary of the total distances in the urban environment for corresponding σ values are summarised in table II.

In the sub-urban environment, with an additional loss of $5\,\mathrm{dB}$, the achievable distance is $283\,\mathrm{m}$ when a $0.001\,\mathrm{m}^2$ size sensor is utilised. The total achievable distance is $503\,\mathrm{m}$ when a $0.01\,\mathrm{m}^2$ sensor is used. For a $0.16\,\mathrm{m}^2$ sensor, the total achievable range is $1000\,\mathrm{m}$. It is observed that this value is the closest to the the total distance achieved utilising the ray tracing technique in the sub-urban environment. Finally, total distances of $1178\,\mathrm{m}$ and $1456\,\mathrm{m}$ are achieved utilising $0.3\,\mathrm{m}^2$ and $0.7\,\mathrm{m}^2$ size sensors. These values are summarised for different σ values in table II.

An analysis is also carried out to determine how the additional loss affects the calculation of the range using the radar equation. Fig. 3 shows the distance the ray is able to travel between the TX and the RX for different values of additional loss. The additional loss makes a significant impact on the achievable distance. Values from $0\,\mathrm{dB}$ to $20\,\mathrm{dB}$ are used to in the graph to represent various use cases. Radar cross section (σ) values vary and are represented by the different curves in Fig. 3. It is observed that the increase in the additional loss decreases the total achievable distance.

VI. Conclusion

In this paper, an analysis was performed to determine the maximum achievable distance between the TX and the RX after reflection from the sensor utilizing ambient LTE-700 signals. This is one of the lowest available frequency band for mobile communications. Furthermore, it was assumed that the TX and RX were operating in the mono-static mode and the sensors are located in their LOS path. The ray tracing approach and the radar equation were utilized to perform simulations in the urban macro-cellular and suburban highway environments using different values for the additional loss. Due to the scarcity of interference, the suburban environment represents the best case scenario in contrast to the urban environment which has multiple sources of interference. Additionally, different values were considered for the radar cross section (which acts as the sensor) to indicate real-world IoT deployment scenarios. It was observed that by using the ray tracing approach, distances of $550\,\mathrm{m}$ and $950\,\mathrm{m}$ were achieved in urban and suburban environments, respectively. Utilising the radar equation it was observed that distances of a few hundred meters are achievable depending on the size of the sensor and the additional loss. The distances achieved by using the ray tracing approach and the radar equation demonstrate that this approach performs well for LOS links in the outdoor environment.

References

[1] H. Stockman, "Communication by means of reflected power," *Proceedings of the IRE*, vol. 36, no. 10, pp. 1196–1204, Oct 1948.

[2] L. Xie, Y. Yin, A. V. Vasilakos, and S. Lu, "Managing rfid data: Challenges, opportunities and solutions," *IEEE Communications Surveys Tutorials*, vol. 16, no. 3, pp. 1294–1311, Third 2014.

[3] V. Liu, A. Parks, V. Talla, S. Gollakota, D. Wetherall, and J. R. Smith, "Ambient backscatter: Wireless communication out of thin air," *SIGCOMM Comput. Commun. Rev.*, vol. 43, no. 4, pp. 39–50, Aug. 2013.

[4] B. Kellogg, A. Parks, S. Gollakota, J. R. Smith, and D. Wetherall, "Wi-fi backscatter: Internet connectivity for rf-powered devices," *SIGCOMM Comput. Commun. Rev.*, vol. 44, no. 4, pp. 607–618, Aug. 2014.

[5] D. Bharadia, K. R. Joshi, M. Kotaru, and S. Katti, "Backfi: High throughput wifi backscatter," *SIGCOMM Comput. Commun. Rev.*, vol. 45, no. 4, pp. 283–296, Aug. 2015.

[6] R. Biswas, J. Sae, and J. Lempiainen, "Power budget for wide area ambient backscattering communications," in *2018 IEEE Vehicular Networking Conference (VNC)*. IEEE, 12 2018.

[7] M. U. Sheikh, R. Duan, and R. Jantti, "Validation of backscatter link budget simulations with measurements at 915 mhz and 2.4 ghz," in *2019 IEEE 89th Vehicular Technology Conference (VTC2019-Spring)*, 2019.

[8] S. H. Choi and D. I. Kim, "Backscatter radio communication for wireless powered communication networks," in *2015 21st Asia-Pacific Conference on Communications (APCC)*, Oct 2015, pp. 370–374.

[9] X. Lu, D. Niyato, H. Jiang, D. I. Kim, Y. Xiao, and Z. Han, "Ambient backscatter assisted wireless powered communications," *IEEE Wireless Communications*, vol. 25, no. 2, pp. 170–177, April 2018.

[10] F. Jameel, I. Khan, and B. Lee, "Simultaneous harvest-and-transmit ambient backscatter communications under rayleigh fading," *EURASIP Journal on Wireless Communications and Networking*, vol. 2019, 12 2019.

[11] N. Van Huynh, D. T. Hoang, X. Lu, D. Niyato, P. Wang, and D. I. Kim, "Ambient backscatter communications: A contemporary survey," *IEEE Communications Surveys Tutorials*, vol. 20, no. 4, pp. 2889–2922, Fourthquarter 2018.

[12] D. Barton, C. Cook, P. Hamilton, and I. ANRO Engineering, *Radar Evaluation Handbook*, ser. Radar Library. Artech House, 1991.

[13] S. Sesia, I. Toufik, and M. Baker, *LTE, The UMTS Long Term Evolution: From Theory to Practice*. Wiley Publishing, 2009.